Enhanced Cell-Seeding into 3-D Scaffolds by Use of Magnetite Nanoparticles for Tissue Engineering

Kazunori Shimizu, Akira Ito, Hiroyuki Honda

Department of Biotechnology, School of Engineering, Nagoya University, Nagoya 464-8603, Japan.
Correspondence to: H. Honda; e-mail: honda@nubio.nagoya-u.ac.jp

Tissue engineering is a promising technology for solving the organ transplantation crisis caused by donor shortage. One approach to tissue engineering is to isolate cells from a small tissue biopsy, expand the cells *in vitro*, and seed them into three-dimensional (3-D) porous biodegradable scaffolds that allow the cells to form a continuous structure via cell adhesion, proliferation and deposition of extracellular matrix (ECM)[1]. In these processes, cell seeding is the first step in constructing the 3-D tissue-like structures. Although cell seeding into scaffolds at high density is closely associated with enhancement of tissue formation in 3-D constructs, effective and high-density cell seeding into 3-D scaffolds is difficult to achieve.[2-4]

In the present study, we developed new methodology of cell seeding into scaffolds, which we termed “Mag-seeding”. Previously, we proposed the novel tissue engineering methodology using magnetite nanoparticles and magnetic force and we termed it as magnetic force based tissue engineering, “Mag-TE”.[5-12] Mag-seeding is based on the Mag-TE having two steps; 1) labeling cells magnetically by magnetite nanoparticles, 2) manipulating the cells by magnetic force. Magnetite nanoparticles are now used in an increasing number of biological and medical applications.[13-16] Based on the fact that high magnetic flux density attracts magnetically labeled cells, magnetite particles have been used for cell sorting. In this study, magnetite cationic liposomes (MCLs) are used to label cells magnetically. MCLs, which are cationic liposomes containing 10-nm magnetite nanoparticles, improve the accumulation of magnetite nanoparticles in target cells via electrostatic interaction between MCLs and the cell membrane.[17]

First of all, the uptake of magnetite nanoparticles by mouse fibroblast cell, NIH/3T3, (FB) and the toxicity of MCLs against FBs were investigated. In the previous studies, MCLs did not show toxicity against any types of cell within the range from 25 to 200 pg/cell and we observed no effect on differentiation of human Mesenchymal stem cells. In the present paper, MCLs were added to FBs at a concentration of 100 pg/cell for magnetic labeling. Fig. 1a showed that uptake peaked at 19 pg magnetite per cell at 4 h after

addition of MCLs. Subsequently, magnetite uptake decreased at 24 h and 48 h after addition of magnetite nanoparticles due to dilution caused by cell proliferation. The growth of FBs in medium containing MCLs (magnetite concentration, 100 pg) was compared with that in medium without MCLs and resulted that MCLs did not inhibit FB growth at the concentration tested (Fig. 1b).

Subsequently, the cell-seeding efficiency by Mag-seeding and static-seeding was compared. Fig. 2 shows a schematic diagram of the cell-seeding methods. In conventional cell seeding (static-seeding), the cell suspension is seeded into small scaffolds using small volumes of highly concentrated cell suspension and the cell suspension flows away with medium flow and few cells remain in the scaffolds. However, in Mag-seeding, magnetic force would be able to attract the magnetically labeled cells to prevent them from flowing away and numerous cells would be able to be seeded into scaffolds because a magnet was placed at the reverse side of the culture dish which a scaffold had been placed on. In addition, technical difficulties in cell seeding are also caused by the size of scaffolds, complex structure of the scaffold and insufficient migration into the scaffolds due to pore size and material, which prolongs the culture period due to a shortage of initially seeded cells.[18-23] Thus, we investigated the cell-seeding efficiency for six kinds of scaffolds which have different size, pore size, materials and so on by Mag-seeding and by static seeding.

Six types of scaffold are listed in Table 1. As shown in Fig. 3a, the cell-seeding efficiency for all scaffolds was enhanced by Mag-seeding using 0.4 T of magnet. The highest cell-seeding efficiency (70.0%) was achieved when cells were seeded into PLA by Mag-seeding. In static-seeding, the cell-seeding efficiencies in Col#1, Col#3 and Col#5 were particularly low (less than 5.0%). On the other hand, the cell-seeding efficiencies in these scaffolds (Col#1, 31.5%; Col#3, 24.8%; Col#5, 19.7%) were markedly improved by Mag-seeding. In particular Col#5, very few cells were detected when seeded by static-seeding (Fig. 3 and 4). The cell suspension poured onto the scaffold might flow away because the apparent size of Col#5 is small (width, 2.9 mm × 2.4 mm; height, 2.1 mm; Table 1). On the other hand, a large amount of cells was observed in Col#5 after Mag-seeding (Fig. 3 and 4), thus suggesting that cells were attracted into scaffold by magnetic force. These results suggest that Mag-seeding could enhance cell-seeding efficiency into scaffolds with any apparent sizes.

Fig. 4 shows the relationship between pore size and cell number in the scaffold. As pore size increased, cell number in the scaffold increased, reaching a plateau of approximately 5000 cells/mm^3 for static-seeding and 12000 cells/mm^3 for Mag-seeding.

Because the apparent scaffold size was particularly small in Col#5 (Table 1), very few cells were detected when the cells were seeded by static-seeding (Figure 4; pore size, 600 μm) because cell suspension poured onto the scaffold flowed away. On the other hand, a substantial amount of cells was detected when the cells were seeded by Mag-TE, thus suggesting that magnetic force facilitates cell seeding.

Histological observation revealed that cells were distributed in the scaffolds both by static-seeding and Mag-seeding, with more cells being observed in the case of Mag-seeding (Fig. 3b). Col#1 exhibited a unique pattern of cell distribution; cells were mostly distributed at the top of the scaffold, possibly due to the small pore size (50 μm). In all other scaffolds, cells seeded by Mag-TE were distributed throughout (data not shown). Therefore, it was revealed that cell-seeding efficiency was dependent on pore size of the scaffold. In static-seeding, cells enter the scaffold due to natural precipitation by gravity. For scaffolds with small pore size, such as Col#1, most of the cells poured onto the scaffold will not enter, and only a small number of cells are seeded within the scaffold. In the present study, magnetic force was applied to cells in order to attract the cells into the scaffold. Mag-seeding allowed a large number of cells to enter the scaffold at all pore sizes tested.

According to the results, it was elucidated that Mag-seeding enhanced the cell-seeding efficiency into scaffolds. Thus, the effects of magnetic force intensity on cell-seeding efficiency were investigated (Table 2). Col#2 and 2 types of magnet (magnetic field intensities of 0.4 T and 1 T) were used in this experiment. Magnetic flux density of the 1 T magnet was approximately 2.5 times higher than that of the 0.4 T magnet. As shown in Table 2, the seeding efficiency by Mag-seeding with the 1 T magnet was 58.9± 6.6%, which was significantly higher than the efficiency by static-seeding (10.8± 6.7%) or by Mag-seeding with the 0.4 T magnet (33.5± 7.1%). These results suggest that the high cell-seeding efficiency achieved by Mag-seeding was by virtue of magnetic force.

In conclusion, high-efficiency seeding of FBs into 3-D porous scaffolds was achieved using the novel Mag-seeding technique, and Mag-seeding may provide a useful and effective cell seeding methodology.

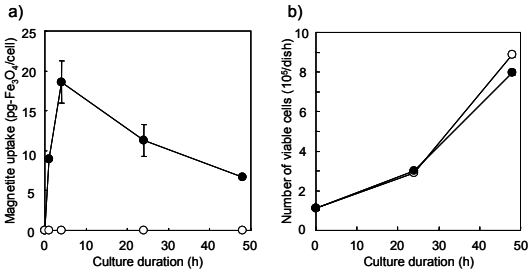

Figure 1. MCL uptake and proliferation of FBs. Magnetic nanoparticle uptake after addition of MCLs (100 pg/cell) was measured by the potassium thiocyanate method (a). Toxicity of MCLs against FBs was examined by cell growth after addition of MCLs (b). Open circles, no MCLs; closed circles, MCLs at 100 pg/cell. Data points represent mean ± SD of duplicate experiments.

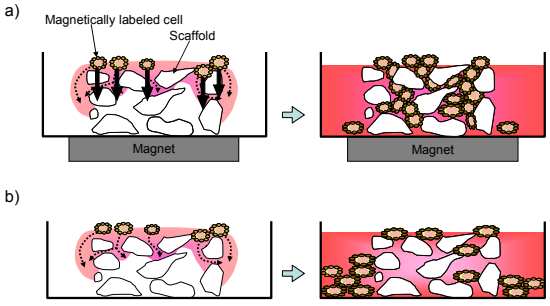

Figure 2. Schematic diagram of Mag-seeding. a) Mag-seeding. b) Static seeding. For Mag-seeding, a magnet is placed at the reverse side of the culture dish and the magnetically labeled cells are attracted by the magnetic force (solid arrow). For static-seeding, the cells are moved by the medium flow (dotted arrow).

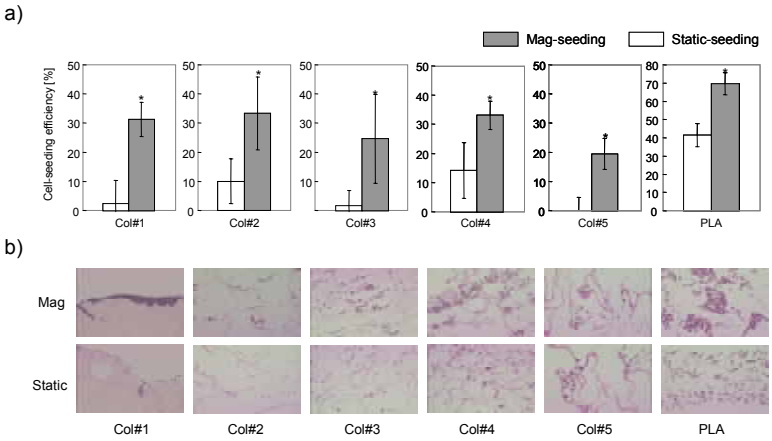

Figure 3. Cell-seeding efficiencies and the histological appearances of cell-seeded scaffolds by Mag-seeding and by static-seeding. a) FBs labeled with MCLs were seeded onto 6 types of scaffold (Col#1~5 and PLA). A 0.4-T magnet was placed under the tissue culture plate and the plate was incubated for 1 h. Open bars, static-seeding; closed bars, Mag-seeding. Data points represent mean ± SD of triplicate experiments. *P< 0.05 against static-seeding (Mann-Whitney rank sum test). b) photographs of cross-section of the cell-seeded scaffolds.

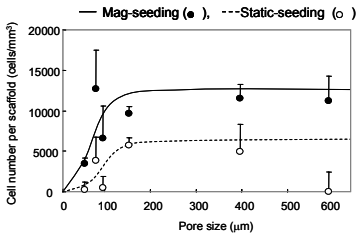

Figure 4. Relationship between pore size and number of cells seeded in each scaffold. Open circles, static-seeding; closed circles, Mag-seeding. Data points represent mean ± SD of triplicate experiments.

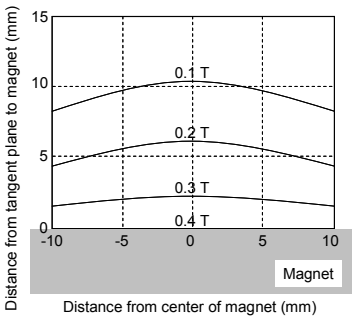

Figure 5. Magnetic flux of 0.4 T magnet. Constant magnetic flux density lines from the surface of the 0.4 T magnet are shown. Magnetic flux was measured using a handheld gauss meter.

Table 1. List of scaffolds used in this study.

Product	[1]Pore size (μm)	Size (mm)	[2]Porosity (%)
Collagen sponge (Col#1)	50 (20-80)	Φ 5.0 x 3.6	97.08 ± 2.15
Collagen sponge (Col#2)	75 (50-100)	Φ 5.0 x 1.3	97.12 ± 0.62
PELNAC (Col#3)	90 (70-110)	Φ 5.0 x 4.1	98.49 ± 0.46
Collagen sponge (Col#4)	400 (300-500)	Φ 5.0 x 3.4	97.91 ± 0.12
Honeycomb (Col#5)	600 (200-1000)	2.9 x 2.4 x 2.1	99.20 ± 0.96
BD 3D OPLA (PLA)	150 (100-200)	Φ 5.0 x 3.6	94.85 ± 0.08

[1] Average diameter (Range of pore size)
[2] Data are mean ± SD, n=3.

Table 2. Effects of intensity of magnetic induction on cell-seeding efficiency.

	Static-seeding (No magnet)	Mag-seeding (0.4T)	Mag-seeding (1T)
Cell-seding efficiency (%)	10.8 + 6.7	33.5 + 7.1	58.9 + 6.6

There was a statistically significant difference between three groups (ANOVA; F= 37.62, P= 0.0004). A post hoc analysis (Bonferroni test) showed significantly higher cell-seeding efficiency of Mag-seeding using a 0.4 T magnet or a 10 T magnet, compared with efficiency of static-seeding (P< 0.05). A significant difference was also observed between cell-seeding efficiency of Mag-seeding using a 10-kG magnet and a 4-kG magnet (P< 0.05).

MATERIALS AND METHODS

Cell and culture

In the present study, NIH/3T3 fibroblast cells (FBs) were used as model cells. FBs were obtained from the American Tissue Culture Collection and were cultured in DMEM-high glucose (Invitrogen, Carlsbad, CA) supplemented with 10% fetal bovine serum (FBS; Sigma, St Louis, MO), 0.1 mg/ml streptomycin sulfate and 100 U/ml potassium penicillin G (Invitrogen), at 37°C in a humidified atmosphere of 5% CO_2 and 95% air.

Scaffolds

The 6 types of scaffold used in this study are shown in Table 1. Five scaffolds (Col#1, 2, 3, 4, 5) were collagen sponges and one was a D,D-L,L polylactic acid (PLA) sponge. Col#1, 2, 3, 4 and PLA were punched into discs having a cylindrical shape of 5 mm in diameter. Col#5 was rectangular in shape and, because it was sufficiently small (width, 2.9 mm × 2.4 mm; height, 2.1 mm), was not punched into a disc. The overall dimensions of each scaffold were measured with calipers. For determining the porosities, scaffolds dry weight in grams were determined with an analytical balance and were then submerged in sterile water for 1 h. Then they were weighed to obtain scaffold wet weight in grams. Percent porosity was determined using the equation:

Percent porosity = {1 – [(scaffold wet weight – scaffold dry weight) / scaffold volume]} × 100

Magnets

Two types of magnet were used in this study; cylindrical neodymium magnets with magnetic inductions of 0.4 T (diameter, 30 mm; height, 15 mm) and 1 T (diameter, 25 mm; height, 200 mm). Figure 5 shows the magnetic fluxes of the 0.4 T magnet. Magnetic fluxes were measured using a handheld gauss meter (F. W. Bell, Orlando, FL).

Preparation of Magnetite cationic liposomes

Magnetite (Fe_3O_4; average particle size, 10 nm) used as the core of the MCLs was kindly donated by Toda Kogyo (Hiroshima, Japan). MCLs were prepared as described previously[17]. Briefly, colloidal magnetite and a lipid mixture consisting of N-(α-trimethylammonioacetyl)-didodecyl-D-glutamate chloride (TMAG, a cationic lipid), dilauroylphosphatidyl-choline (DLPC) and dioleoylphosphatidyl-ethanolamine (DOPE) in a

1:2:2 molar ratio were used. The average MCL particle size was 150 nm and this was measured using a dynamic light scattering spectrophotometer (FRAR 1000, Otsuka Electronics, Osaka, Japan).

MCL uptake by cells

Uptake of MCLs by FBs was examined as previously reported[14]. Briefly, FBs (1 x 10^5 cells) were seeded into a 60-mm cell culture dish (Asahi Techno Glass, Chiba, Japan) with 5 ml of culture medium containing MCLs (net magnetite concentration, 100 pg/cell) and were incubated. To assay magnetite uptake, cells were sampled periodically and the iron concentration was measured using the potassium thiocyanate method. To examine the effects of MCL uptake on cell growth, cells were counted using the dye-exclusion method with trypan blue.

Cell seeding experiments

FBs were cultured in a 100-mm cell culture dish (Asahi Techno Glass) to subconfluence and were then incubated for 4 h with 10 ml of culture medium containing MCLs (net magnetite concentration, 100 pg/cell). Labeled FBs were enzymatically detached from the dish using trypsin (Invitrogen). Magnetically labeled FBs were centrifuged at 1000 rpm for 5 min and resuspended in culture medium. Magnetically labeled FBs were counted using the dye-exclusion method with trypan blue and were adjusted to 1.0 x 10^7 cells/ml. Scaffolds were hydrated in culture medium for 4 h at 37°C in a humidified atmosphere of 5% CO_2 and 95% air, and were then placed in the well of 24-well tissue culture plates. For Mag-seeding, a magnet was placed at the reverse side of the 24-well tissue culture plate in order to provide magnetic force vertical to the plate. As a control experiment, no magnet was placed, which we refer to as static-seeding. Aliquots of 100 μl of magnetically labeled cell suspension (1.0 x 10^7 cells/ml) were poured onto the hydrated scaffolds placed in the wells of 24-well cell culture dish. A schematic diagram of Mag-seeding is shown in Figure 2B. After a 1-h incubation period, scaffolds were washed twice with PBS in order to remove unattached cells from the scaffolds. To investigate seeding efficiency, unattached cells were collected and counted using the dye-exclusion method with trypan blue. Cell-seeding efficiency was determined by the equation:

Percent cell-seeding efficiency = [1 – (number of unattached cells / number of seeded cells)] × 100

where, the number of seeded cells was 1.0 × 10^6 cells.

Statistical analysis

The data list was exported to the statistics software package WinSTAT (LIGHTSTONE, Tokyo, Japan) for further analysis. Comparisons of parameters among the three groups were made using an analysis of variance (ANOVA) followed by Bonferroni test. Comparisons of parameters between two groups were made by Mann-Whitney rank sum test. $P< 0.05$ was considered significant.

Histological evaluation

After cell seeding, scaffolds were washed twice with PBS, fixed in 10% formalin solution and embedded in paraffin. Thin (4 μm) slices were cut and stained with hematoxylin and eosin.

REFERENCES

1. Langer R, Vacanti JP. Tissue engineering. Science 1993;260(5110):920-6.
2. Freed LE, Langer R, Martin I, Pellis NR, Vunjak-Novakovic G. Tissue engineering of cartilage in space. Proc Natl Acad Sci U S A 1997;94(25):13885-90.
3. Holy CE, Shoichet MS, Davies JE. Engineering three-dimensional bone tissue in vitro using biodegradable scaffolds: investigating initial cell-seeding density and culture period. J Biomed Mater Res 2000;51(3):376-82.
4. Carrier RL, Papadaki M, Rupnick M, Schoen FJ, Bursac N, Langer R, Freed LE, Vunjak-Novakovic G. Cardiac tissue engineering: cell seeding, cultivation parameters, and tissue construct characterization. Biotechnol Bioeng 1999;64(5):580-9.
5. Ito A, Takizawa Y, Honda H, Hata K, Kagami H, Ueda M, Kobayashi T. Tissue engineering using magnetite nanoparticles and magnetic force: heterotypic layers of cocultured hepatocytes and endothelial cells. Tissue Eng 2004;10(5-6):833-40.
6. Ito A, Hibino E, Honda H, Hata K, Kagami H, Ueda M, Kobayashi T. A new methodology of mesenchymal stem cell expansion using magnetic nanoparticles. Biochem Eng J 2004;20:119-125.
7. Ito A, Hayashida M, Honda H, Hata K, Kagami H, Ueda M, Kobayashi T. Construction and harvest of multilayered keratinocyte sheets using magnetite nanoparticles and magnetic force. Tissue Eng 2004;10(5-6):873-80.
8. Ito A, Ino K, Kobayashi T, Honda H. The effect of RGD peptide-conjugated magnetite cationic liposomes on cell growth and cell sheet harvesting. Biomaterials

2005;26(31):6185-93.

9. Ito A, Ino K, Hayashida M, Kobayashi T, Matsunuma H, Kagami H, Ueda M, Honda H. Novel methodology for fabrication of tissue-engineered tubular constructs using magnetite nanoparticles and magnetic force. Tissue Eng 2005;11(9-10):1553-61.
10. Ito A, Hibino E, Shimizu K, Kobayashi T, Yamada Y, Hibi H, Ueda M, Honda H. Magnetic force-based mesenchymal stem cell expansion using antibody-conjugated magnetoliposomes. J Biomed Mater Res B Appl Biomater 2005;75(2):320-7.
11. Ito A, Hibino E, Kobayashi C, Terasaki H, Kagami H, Ueda M, Kobayashi T, Honda H. Construction and delivery of tissue-engineered human retinal pigment epithelial cell sheets, using magnetite nanoparticles and magnetic force. Tissue Eng 2005;11(3-4):489-96.
12. Shimizu K, Ito A, Lee JK, Yoshida T, Miwa K, Ishiguro H, Numaguchi Y, Murohara T, Kodama I, Honda H. Construction of multilayered cardiomyocyte sheets using magnetite nanoparticles and magnetic force. Biotechnol Bioeng 2006 in press
13. Miltenyi S, Muller W, Weichel W, Radbruch A. High gradient magnetic cell separation with MACS. Cytometry 1990;11(2):231-8.
14. Moore LR, Zborowski M, Sun L, Chalmers JJ. Lymphocyte fractionation using immunomagnetic colloid and a dipole magnet flow cell sorter. J Biochem Biophys Methods 1998;37(1-2):11-33.
15. Radbruch A, Mechtold B, Thiel A, Miltenyi S, Pfluger E. High-gradient magnetic cell sorting. Methods Cell Biol 1994;42 Pt B:387-403.
16. Lewin M, Carlesso N, Tung CH, Tang XW, Cory D, Scadden DT, Weissleder R. Tat peptide-derivatized magnetic nanoparticles allow in vivo tracking and recovery of progenitor cells. Nat Biotechnol 2000;18(4):410-4.
17. Shinkai M, Yanase M, Honda H, Wakabayashi T, Yoshida J, Kobayashi T. Intracellular hyperthermia for cancer using magnetite cationic liposomes: in vitro study. Jpn J Cancer Res 1996;87:1179-1183.
18. Kim BS, Putnam AJ, Kulik TJ, Mooney DJ. Optimizing seeding and culture methods to engineer smooth muscle tissue on biodegradable polymer matrices. Biotechnol Bioeng 1998;57(1):46-54.
19. Bruinink A, Siragusano D, Ettel G, Brandsberg T, Brandsberg F, Petitmermet M, Muller B, Mayer J, Wintermantel E. The stiffness of bone marrow cell-knit composites is increased during mechanical load. Biomaterials 2001;22(23):3169-78.
20. Li Y, Ma T, Kniss DA, Lasky LC, Yang ST. Effects of filtration seeding on cell density, spatial distribution, and proliferation in nonwoven fibrous matrices. Biotechnol Prog

2001;17(5):935-44.

21. Xiao YL, Riesle J, Van Blitterswijk CA. Static and dynamic fibroblast seeding and cultivation in porous PEO/PBT scaffolds. J Mater Sci Mater Med 1999;10(12):773-7.

22. Vunjak-Novakovic G, Radisic M. Cell seeding of polymer scaffolds. Methods Mol Biol 2004;238:131-46.

22. Shimko DA, Shimko VF, Sander EA, Dickson KF, Nauman EA. Effect of porosity on the fluid flow characteristics and mechanical properties of tantalum scaffolds. J Biomed Mater Res B Appl Biomater 2005.